https://doi.org/10.5194/gi-2020-17
Preprint. Discussion started: 24 July 2020

Geoscientific Instrumentation Methods and Data Systems Discussions
Open Access
EGU

Ground penetrating radar inspection for Subsurface Historical Structures at Baptism (El-Maghtas) site, Jordan

[(1)]AbdEl-Rahman Aqel Abueladas[*], [(1)]Emad Akawwi

[(1)]Surveying and Geomatics Department, Faculty of Engineering, Al-Balqa Applied University, Al-Salt 19117, Jordan.

** Corresponding author e-mail: aabueladas@bau.edu.jo, Tel: +962 0791709827, Fax:+962 5 3530465*

Abstract

The Baptism (El-Maghtas) site located north to the Dead Sea at the eastern bank of the Jordan River. There are many excavations in the surrounding area revealed different archaeological remains which indicates the location "John the Baptist". He lived and preached in the early 1st Century C.E. who is famous for John the Baptist baptized Jesus. The archaeological excavations reveals walls, antiquities, ancient water system includes such conduits, pools, and ancient pottery pipe. The Ground Penetrating Radar (GPR) survey was carried out at selective locations along parallel profiles at the study using a Subsurface Interface Radar System (SIRvoyer-20) with either 400 MHz or 900 MHz mono-static shielded antennas manufactured by Geophysical Survey Systems Inc to delineate possible shallow archaeological material at shallow depth. The GPR radar-gram profiles revealed different subsurface anomalies across all sites. At John the Baptist Church site buried wall were detected along profiles, the GPR survey recognized shallow wall and shallow buried channel at the pools site. At Elijah's Hill site the GPR data confirmed the extension of an ancient pottery pipe. Basically the clear diffraction hyperbola anomaly related to the ancient pottery pipe could be discriminated from the two dimension profiles. The GPR data was displaced using three dimension imaging to define the horizontal and the vertical extent of the pipe.

Keywords: Jordan River, Baptism, Archaeological remains, pottery pipe, Ground Penetrating Radar.

https://doi.org/10.5194/gi-2020-17
Preprint. Discussion started: 24 July 2020


Geoscientific Instrumentation Methods and Data Systems Discussions
Open Access
EGU

1 Introduction

Principally the Baptism Site is situated at about eight kilometers far away from the northern corner of the Dead Sea at the eastern bank of the Jordan River (Fig. 1).

Observing that the excavation of the buried archaeology, artifacts and antiquities has been carried out through old traditional random methods like coring, auguring and shovel testing; actually these are a time consuming and a labor acute procedure. The traditional way to identify the presences of any artifacts is to perform a lot of exploratory digging, adding an enormous waste of time and expense.

The site located at arid environments where is localized large number of archaeological remains of various age, origin and size in variable geological–archaeological media (Eppelbaum et al., 2010). The complex soils of the site are complicated associated with vegetation factors in some site complicates accessibility of ground penetrating radar survey (Eppelbaum and Khesin, 2001; Eppelbaum et al., 2010).

GPR is a high resolution instrument that sends electromagnetic (EM) waves and determines the location of reflected energy. GPR has become an accepted tool for various fields, including archaeological, engineering and construction, geological, glaciological, environmental, and forensic science (Neal, 2004). GPR is a high-resolution method uses EM waves in the frequency band of 10-1000 MHz to picture subsurface soil and structure; the advantage of using EM waves with relatively short wavelength signals spectrum is the ability to map small objects at shallow depths. The GPR methodology has been successfully utilized to locate antiquities in urban and arid settings (Vaughan, 1986; Sternberg and McGill, 1995; Cacione et al., 1996; and Basile et al., 2000). On the other hand the ground penetrating radar (GPR) approved to be a unique high-resolution tool to

https://doi.org/10.5194/gi-2020-17
Preprint. Discussion started: 24 July 2020


Geoscientific Instrumentation Methods and Data Systems Discussions
Open Access
EGU

offer a solution to these problems (Vaughan, 1986). The results could be used to identify anomalous areas for excavation, and that will direct the excavation operations to the highest potential areas (Cacione, 1996).

The main objective of this study is to carry out a ground-penetrating radar (GPR) as noninvasive nondestructive tool to obtain information about the existence of archaeological features in the shallow subsoil and to image the depth and extension of a buried ancient pottery pipe which apart of it has been already excavated.

In addition, the data presentations do play a significant role in the archaeological inspections since they assemble a view of the location, and fix on the size and the extension of the anomalies (Basile et. al., 2000). The GPR survey was carried out at three different sites to indicate any shallow anomalies.

2 Historical Background

Baptism (El-Maghtas) site is a prehistoric area. Considerably it is one of the most important archaeological discoveries of the early Christianity; happened to be located in Jordan valley to the western part of Jordan. It located about 50 km far from the west of Amman (Capital of Jordan). Furthermore a settlement of Bethany in Jordan; where John the Baptist lived in the time of Christ; tends to be part of Baptism (El-Maghtas) prehistoric area.

However; John the Baptist's settlement is connected to several biblical incidents: the baptism of Jesus which took place in Bethany, Joshua's crossing of the Jordan River, the last days of Moss, and the Prophet Elijah's crossing of Jordan and been ascended to heaven in a whirlwind upon a chariot on horses of fire (two kings 2:5-14). Almost for 2000 years, the local church tradition and the pilgrims used to identify the small hill at

https://doi.org/10.5194/gi-2020-17
Preprint. Discussion started: 24 July 2020


Geoscientific Instrumentation Methods and Data Systems Discussions
Open Access
EGU

the center of Bethany as the site from which Elijah was raised to paradise, and the site became famous of Elijah's Hill (or Tell Mar Elias, or Jabal Mar Elias), where the Jordan River located about 2 km far away to the west of the site.

The settlement of Bethany and the surrounding region in Jordan were also famous during different ancient periods as Ainon, Saphaphas, Bethanin and Bethabra (Beit el-Obour, or house of crossing); however the Arabic language bibles tend to call it Beit 'Anya, thus, today the entire region between Bethany and the Jordan River is called El-Maghtas (the place of immersion or baptism).

Apparently the current work in the area was able to identify numerous structures, monastic complexes, churches, caves, a system of water pipes and channels to carry water and other facilities from Roman and Byzantine era (4^{th} to 8^{th} centuries C.A.) (Waheeb, 2001). Effectively the archaeological dig has revealed a settlement from the time of Jesus and John the Baptist (early 1^{st} century C.A.).

In brief, the existing of the excavated water constructions like (aqueducts, pools, cisterns, and pottery pipe) is a fact witness of the complexity of the water system at the area. Where, the settlers in the past were limited to depend upon the rainwater collection and springs. Consequently, the Roman and Byzantine used to divert the water from nearby Wadi using conduit and pottery pipes to fill the pools and cisterns as reservoirs (Waheeb, 2003).

3 GPR concepts

Ground penetrating radar (GPR) is a high-resolution method of picturing subsurface structures using electromagnetic (EM) waves in the frequency band from 10 MHz to one GHz. The benefit of using (EM) waves is that signals of relatively short wavelength can

https://doi.org/10.5194/gi-2020-17
Preprint. Discussion started: 24 July 2020


Geoscientific Instrumentation Methods and Data Systems Discussions
Open Access
EGU

be generated and directed to the subsurface to map anomalous vary in there electrical properties, in many aspects.

Discriminatory feature of GPR is that the method is simple to use and is neither invasive nor destructive; this makes it appropriate for use also in urban areas and archaeological sites.

The propagation of EM energy in the medium is mainly controlled by dielectric permittivity (ε), electrical conductivity (σ) and magnetic permeability (μ). At high frequencies the electric polarization properties control the conductive properties for many earth materials. Dielectric permittivity depends on the applied frequency and altering electric field.

In this region the velocity of propagation keeps constant and the radar signal is not scattered by frequency-dependant velocity. In low-loss earth materials the radar signal velocities are related to relative permittivity.

$V = C/\sqrt{\varepsilon_r \mu_r}$ where $\varepsilon_r = \varepsilon/\varepsilon_0$ is the ratio of the dielectric permittivity of the medium to the dielectric permittivitty of free space.

$\mu_r = \mu/\mu_0$ is the relative magnetic permeability of the medium, and $C = 3 \times 10^8$ m/sec is the velocity of EM in the free space.

Since the μ_r is close to unity for most row materials, radar velocity is primarily controlled by ε_r and the dielectric constant. Dielectric constant across an interface cause part of an impinging radar pulse to be reflected the radar signal amplitude is decreased at the reflecting borders relying on the contrast and the thickness of the layer. The reflection-coefficient (K) at a half-space for a normal incident signal is given by

$K = (V_{\varepsilon r2} - V_{\varepsilon r1}) / (V_{\varepsilon r2} + V_{\varepsilon r1})$

https://doi.org/10.5194/gi-2020-17
Preprint. Discussion started: 24 July 2020


Geoscientific Instrumentation Methods and Data Systems Discussions

Where ε_{r1} and ε_{r2} are the relative permittivity of the two media across the interface.

The attenuation of a radar wave and its depth of penetration depend on the electrical conductivity and dielectric constant of the media through which the wave propagates can be reduced for the case of low-loss media $\sigma / \varepsilon_w << 1$ to a simple form $\alpha = (\sigma / 2) \times (\mu/\varepsilon_r)^{0.5}$.

Where α donates the attenuation constant and σ merges both the D.C. conductivity and dielectric losses. The horizontal resolution links to the ability to detect reflector location in space or time, which is a function of the pulse width. The vertical resolution increases with an increase in the frequency. The vertical resolution is also controlled by wavelength (λ) (Knapp, 1990) which is a function of velocity and frequency:

$\lambda = v / f$

The best vertical resolution can be obtained by using one-quarter of the dominant wavelength (Sheriff and Geldart, 1995).

4 GPR Survey

4.1 Data Acquisition

Continuous GPR survey was conducted utilizing SIRvoyer-20 produced by Geophysical Survey System (GSSI). The 900 MHz and 400 MHz frequency antennas were used in this study. A total of 88 meters of GPR survey were collected along 11 profiles at three different sites. The first survey was carried out at the site located north of John the Baptist Church, the second one located south of the pools, and the third one located at South Elijah's Hill. Five profiles were carried out at the last site (Fig. 1). At the second and third sites, the survey was carried out by using 900 MHz antenna.

https://doi.org/10.5194/gi-2020-17
Preprint. Discussion started: 24 July 2020


Geoscientific Instrumentation Methods and Data Systems Discussions
Open Access
EGU

4.2 Data processing

Minimum data processing was applied utilizing GSSI RADAN V software package from GSSI. Horizontal and vertical high pass and low pass filters were used to enhance the radar cross section. Additional processing to convert two-way travel times along the section to depth in meter applying average radar wave velocity. Data were stacked in horizontal direction along long profiles.

Furthermore, the 900 MHz antenna has been used throughout the survey with data parameters:

- Range: 15 and 50 ns, IIR filter *f*/4 to 2*f*; where (*f*) is the antenna center frequency.
- Gain function automatic, transmit rate of 50 scan/s, 512 samples and 16 A/D conversion.
- In processing of the exhibited waveforms, horizontal and vertical high and low pass filters that have been applied to eliminate the surplus noise off the GPR signal. Then the Data were showed, edited, while both of the horizontal and vertical scales were attuned before processing (Abueladas, 2005).
- Time-zero correction was adjusted to the raw GPR data which were then managed by using range and display gain, filtering, color conversion, and migration procedures (Aqeel et al., 2014).
- The obtained GPR data were processed and presented as 2-D depth cross sections providing a logical vertical/horizontal resolution for the upper 2 m of the inspected site (Odah et al., 2013)
- Attenuation generally reduces the radar signal with increased travel time. Therefore, it is important to increase the weaker signals at greater receiver arrivals. The gain or

https://doi.org/10.5194/gi-2020-17
Preprint. Discussion started: 24 July 2020


Geoscientific Instrumentation Methods and Data Systems Discussions

the strength of the signal is based on time-variant scaling. Gains are applied to preserve relative amplitudes and for advanced data processing.

- Calculation of the subsurface radar-wave velocity is essential to convert the TWT of the reflected signal to the true depth of the reflector (Annan, 2003; Fisher et al., 1992). However, this study calibrated the velocity according to the known depth aligned with the top of excavated pipe near the study area.

The dielectric permittivity of the various areas is obtained using an approximation of the reflection delay formula, which connects wave velocity (v), to measured depth (x), the recorded two-way travel time (t), the relative permittivity (ε_r), and the free-space velocity (c) (Gracia et.al., 2008)

$$\varepsilon_r = \left(\frac{c}{v}\right)^2 = \left(\frac{ct}{2x}\right)^2$$

The computed near surface average velocity was 0.12 m/ns (Fig. 2).

5 Results and discussions

A total of three continuous parallel profiles up to 12 m long were recorded at site 1. The separation between the north-south adjacent profiles was a constant 1 m (Fig. 1).

The 400 MHz antenna radar gram along profile 4001 shows a clear large discontinuous anomaly is pictured along the profile with approximately depth 1.2 m, which interpreted as a discontinuous buried wall (Fig. 3).

Along profile 4002 which is located to the north, the same anomaly but at shallower depth was detected (Fig. 4).

These anomalies caused by dissimilarities in wave velocity at the point of contact between dissimilar materials, their depths, and extensions indicate possible buried wall which direction south-north. No other anomalies were detected within profile 4003.

https://doi.org/10.5194/gi-2020-17
Preprint. Discussion started: 24 July 2020


Geoscientific Instrumentation Methods and Data Systems Discussions
Open Access
EGU

A 900 MHz antenna profile 9001 was acquired along a W-E and located at site 2 (Fig. 1). Radar gram shows one main anomaly at a depth of 0.25 m located at a distance between 1 and 3 m, which interpreted as a shallow buried wall (Fig. 5). The 3 meter wide depression at the end of the profile may be correlates to shallow buried channel.

Profile 9002 is 10 m long and runs parallel to profile 9001, approximately 1 m to the north of profile 9001 (Fig. 1). The same anomaly and depression were detected along this profile located to the north (Fig. 6).

The 12 m length profile 9003 is located to the north of profile 9002 closer to the pool (Fig. 1). The radar profile shows anomaly between markers 2 and 5 m at an approximate depth of 0.25 m, which interpreted as a buried wall (Fig. 7). The bottom of the depression along this profile is deeper and the width is lesser than the southern profiles.

Site 3 was a rectangle of 2 by 5 m applied to a flat area near Elijah's Hill. The uni-directional survey was conducted along five profiles oriented approximately N-S with spaced 0.5 m apart using 900 MHz to the east of the excavated pottery pipe (Fig. 1). The purpose of the survey is to trace the depth and extension of an ancient buried pottery pipe, which was one of water constructions of the ancient water system. The most parts of the ancient pipe were destroyed by human activities, while other sections were excavated at parts of the study area.

A GPR profile 1 was collected perpendicular to the trend of the excavated pottery pipe just east of the excavation using a 900 MHz antenna (Fig. 1). The hyperbolic-shaped anomaly appears at mark 2.5 and about 0.55 m deep represents the location of the buried pipe (Fig. 8).

https://doi.org/10.5194/gi-2020-17
Preprint. Discussion started: 24 July 2020


Geoscientific Instrumentation Methods and Data Systems Discussions
Open Access
EGU

229 Actually, the main anomalies appeared as diffraction hyperbolas shape with high
230 amplitudes observed at distance 2.5 m and 0.55 m deep along all the 2D ground
231 penetrating radar cross section.
232 Generally targets of interest are generally easier to identify. On three-dimensional data
233 than on conventional the two dimensional profile lines. The 3D GPR data were generated
234 from 2D and displayed using 3D-visualisation techniques, which is primary importance
235 in archaeological applications.
236 The 3D perspective view of processed profiles via high pass and low pass vertical and
237 horizontal filters together with the migration technique that illustrates the location of the
238 pottery pipe (Fig. 9) (Whiting, 2001; Fisher et al., 1992a).
239 The depth slices with different depths (0, 0.25, 0.55, 0.75 m) generated from 3D plot are
240 presented in figure 10. The main anomaly observed with W-E direction at depth slice
241 0.55 mbs (meter below surface) correspond to the anomaly of the pottery pipe. Thus, the
242 depth slices provide good information about the exact location and extension of the pipe.
243 The multiple slices view along the y direction at distances (0, 1 and 2 m) determines the
244 extension of the pipe anomaly along the y direction (Fig. 11).
245 The 3D section (chair view) applying that the X= 2.5 m, Y= 0.85 m, and Z= 0.55 shows
246 clearly the depth and the E-W extension of the pipe perpendicular to the X position and
247 the depth of the top of pipe detect by the Z position (Fig. 12). The results of this study
248 showed that many of the subsurface structures were recognized by using the GPR.
249 Subsurface walls were determined. Different subsurface channels were found. The
250 locations of these channels were determined. The flow directions also of these channels

https://doi.org/10.5194/gi-2020-17
Preprint. Discussion started: 24 July 2020


Geoscientific Instrumentation Methods and Data Systems Discussions
Open Access
EGU

were identified from west to east of the study area. Fig. 13 shows the location map of GPR anomalies and their interpretation.

6 Conclusions

Ground penetrating radar (GPR) is a powerful, nondestructive, noninvasive geophysical near surface tool for archaeological surveying. GPR has been used successfully to detect the several shallow anomalies in El-Maghtas Site. The flat topography the absence of archaeological remains at the surface at survey sites allow to image good quality GPR profiles. The high frequency 900 MHz antenna can be used for small size of the archaeological objects located at shallow depth. It is clear that the 3D measurements give better results than the 2D ones, as can be seen from the results. Generally, the survey objects include the identification and mapping of covered walls, channel, and the extension of ancient pottery pipe.

However, the vertical sections, depth slices, 3D images, were used to locate the anomalies using spatial extent 3D survey allow precise detection of the anomaly throughout the entire data that constructed after advanced processing include migration. Using three-dimensional GPR imaging successfully detect the 0.55 m depth and the E-W extension direction of the pottery pipe in El-Maghtas Site.

The clear displacement in the buried wall and the buried channel in site 2 may be caused by shallow fault.

The outcome results can be used to lead any future excavations.

https://doi.org/10.5194/gi-2020-17
Preprint. Discussion started: 24 July 2020

Geoscientific Instrumentation Methods and Data Systems Discussions
Open Access
EGU

Acknowledgements

The authors would thanks Ministry of high education and scientific research for their fund and support through out to the project. We would like also to thanks Eng. Bah El-Madani the former Baptism site Commission Director and his assistant Eng Rostom Mkhjian for their help. We are also grateful to the technicians, Ibrahim Aldabas, Mohamed Aqrabawi, and Ziad Heyassat the employees of (BAU) for their efforts during data acquisition in the field work. We thank very much the anonymous reviewers and the editor for their constructive critics and comments of this manuscript.

References

Abueladas, A.: Ground Penetrating Radar Investigations of Active Faults and Antiquities along the
Dead Sea Transform in Aqaba and Taba Sabkha, Jordan, master thesis, University of Missouri-Kansas City, U.S.A, 71 pp., 2005.

Annan, AP.: GPR principles, procedures and applications: Sensors and Software In, 2003.

Aqeel, A., Anderson, N., and Maerz, N.: Mapping sub-vertical discontinuities in rock cuts using a 400-
MHz ground penetrating radar antenna, Arab J Geosci 7(5), 2093–2105, https://doi.org/10.1007/s12517-013-0937-y, 2014.

Basile, L., Carrazzo, MT, Negra, S., Nuzzo, S., Quarta, L., and Villani, A.V.: A ground-penetrating radar
survey for Archaeological investigations in an urban area (Lecce, Italy), Journal of Applied Geophysics, 44, 15-32, https://doi.org/10.1016/S0926-9851(99)00070-1, 2000.

Cacione, JM.: Radar simulation for archaeological applications: Geophysical Prospecting, 44, 871-888,
https://doi.org/10.1111/j.1365-2478.1996.tb00178.x, 1996.

Eppelbaum, L.V., and Khesin, B.E.: Disturbing factors in geophysical investigations at archaeological sites
and ways of their elimination. In: Transactions of the IV Conference on Archaeological Prospection, Vienna, Austria, 19-23 September 2001, 99–10, 2001

Eppelbaum, L.V., Khesin, B.E. and Itkis, S.E.: Archaeological geophysics in arid
environments: Examples from Israel, Journal of Arid Environments, 74, 849-860,
https://doi.org/10.1016/j.jaridenv.2009.04.018, 2010.

Gracia, V., Garcı, F., Pujades, L., Drigo, R., and Capua, D.: GPR survey to study the restoration of a Roman monument, Journal of Cultural Heritage, 9, 89-96, https://doi.org/10.1016/j.culher.2007.09.003, , 2008.

Fisher, E.: Examples of reverse-time migration of single-channel, ground penetrating radar profiles. Geophysics, 57, 577-586, https://doi.org/10.1190/1.1443271, 2006.

https://doi.org/10.5194/gi-2020-17
Preprint. Discussion started: 24 July 2020

312 Knapp, R. W.: Vertical resolution of thick beds, thin beds and thin-bed cyclothems,
313 Geophysics, 55, 1183-119, https://doi.org/10.1190/1.1442934, 1990.
314 Neal, A.: Ground-penetrating radar and its use in sedimentology: principles, problems
315 and progress, Earth-Science Reviews, 6, 261–330,
316 https://doi.org/10.1016/j.earscirev.2004.01.004, 2004.
317 Odah, H., Ismail, A., Elhemaly, I., Anderson, N., Abbas, A., and Shaaban, F.:
318 Archaeological exploration using magnetic and GPR methods at the first court of
319 Hatshepsut Temple in Luxor, Egypt, Arab J. Geosci, , 6, 865–871,
320 https://doi.org/10.1007/s12517-011-0380-x, 2014.
321 Sheriff, R. E., and Geldart, L. P.: Reflection field methods, Cambridge University Press,
322 England, 1995.
323 Sternberg, B. K., McGill, J. W.: Archaeology studies in southern Arizona using ground
324 penetrating radar. Journal of Applied Geophysics, 33, 209-225,
325 https://doi.org/10.1016/0926-9851(95)90042-X, 1995.
326 Vaughan C. J.: Ground penetrating radar survey used in archaeological investigations.
327 Geophysics, 51, 595-604, https://doi.org/10.1190/1.1442114., 1986.
328 Waheeb, M (2003) Recent Discoveries in the Bethany Beyond Jordan in Jordan Valley.
329 ADAJ 47:243-246.
330 Waheeb M (2001) Archaeological Excavations at the Baptism Site, Bethany Beyond the
331 Jordan. Bible and Spade 14(2):43-53.
332 Whiting, B, McFarland, D., and Hackenberger, S.: Thee-Dimensional GPR study of a
333 prehistoric site in Barbados, West Indies. Journal of Applied Geophysics, 47, 217-226,
334 https://doi.org/10.1016/S0926-9851(01)00066-0, 2001.

https://doi.org/10.5194/gi-2020-17
Preprint. Discussion started: 24 July 2020

Geoscientific Instrumentation Methods and Data Systems Discussions
Open Access
EGU

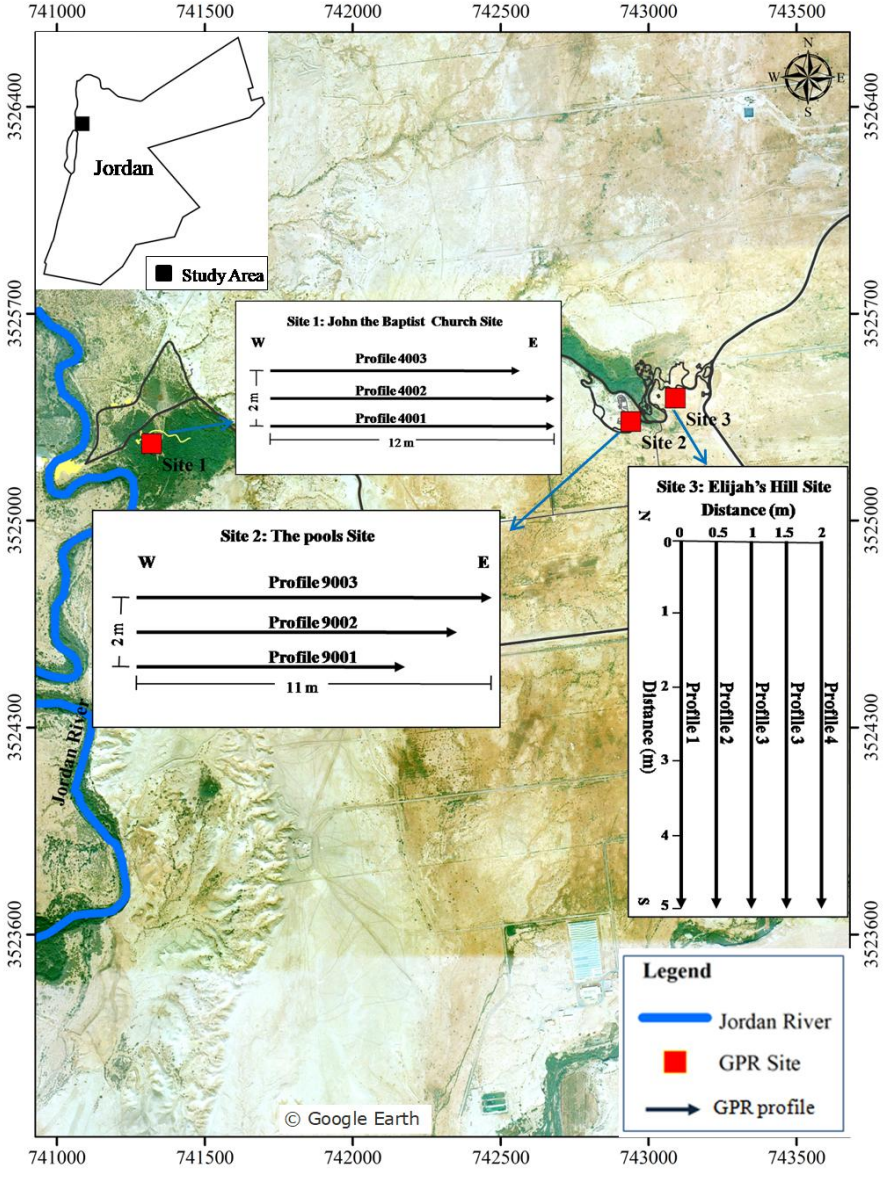

335
336 Figure-1
337

https://doi.org/10.5194/gi-2020-17
Preprint. Discussion started: 24 July 2020

Geoscientific Instrumentation Methods and Data Systems Discussions
Open Access
EGU

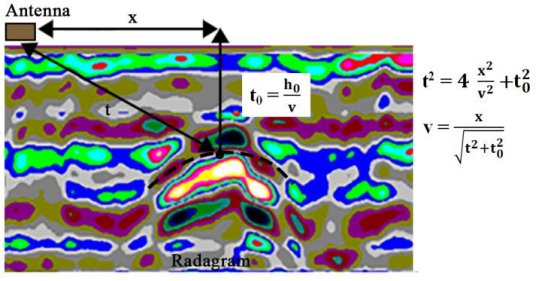

338
339
340 Figure-2
341
342

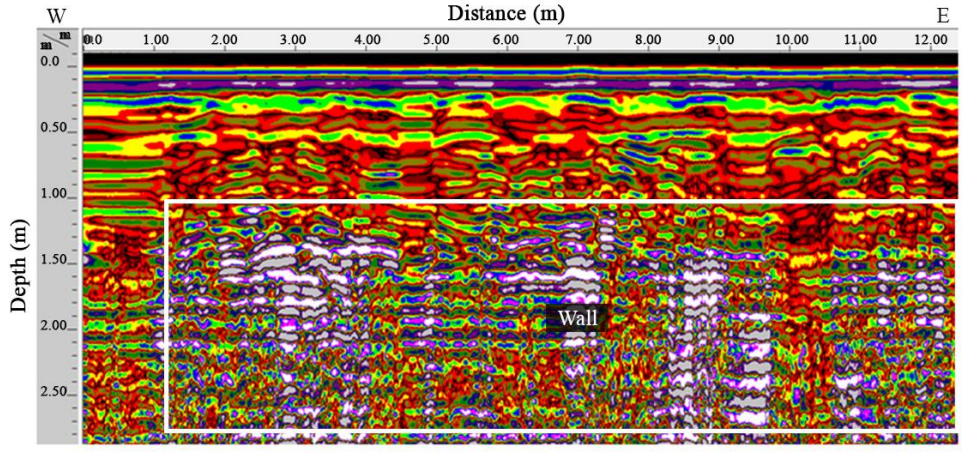

343
344 Figure-3

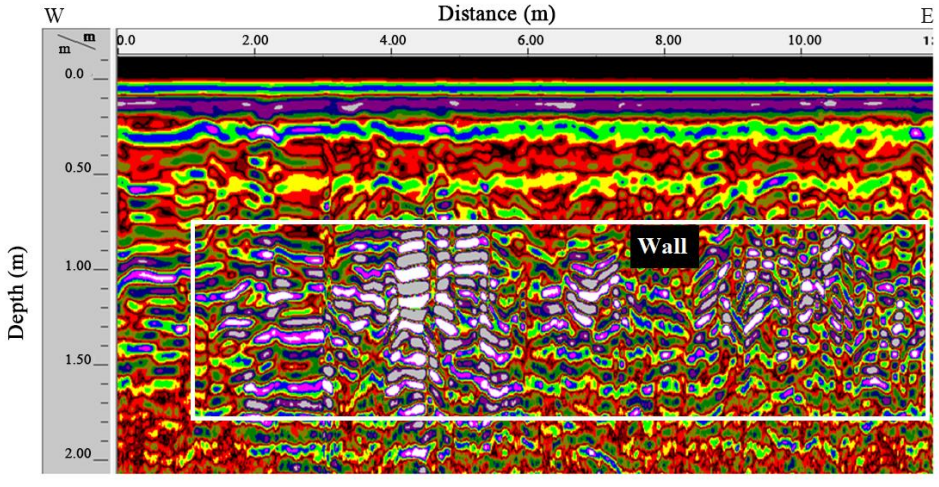

345
346 Figure-4

https://doi.org/10.5194/gi-2020-17
Preprint. Discussion started: 24 July 2020

Geoscientific Instrumentation Methods and Data Systems Discussions
Open Access
EGU

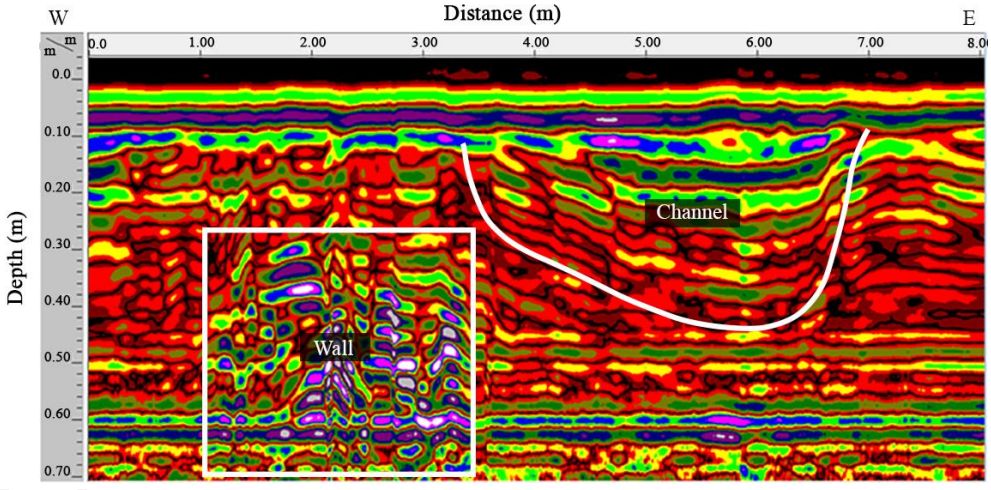

Figure-5

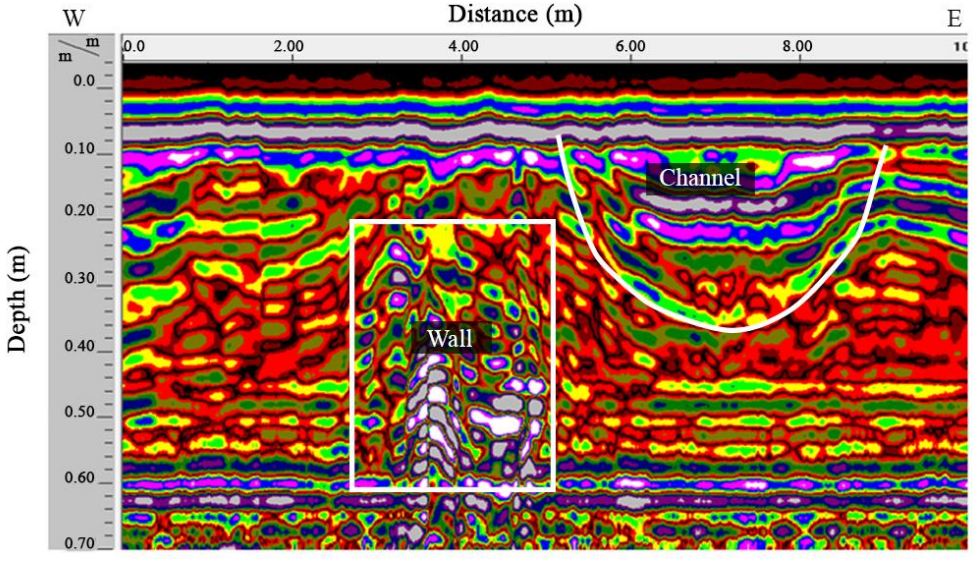

Figure-6

https://doi.org/10.5194/gi-2020-17
Preprint. Discussion started: 24 July 2020

Geoscientific Instrumentation Methods and Data Systems Discussions
Open Access
EGU

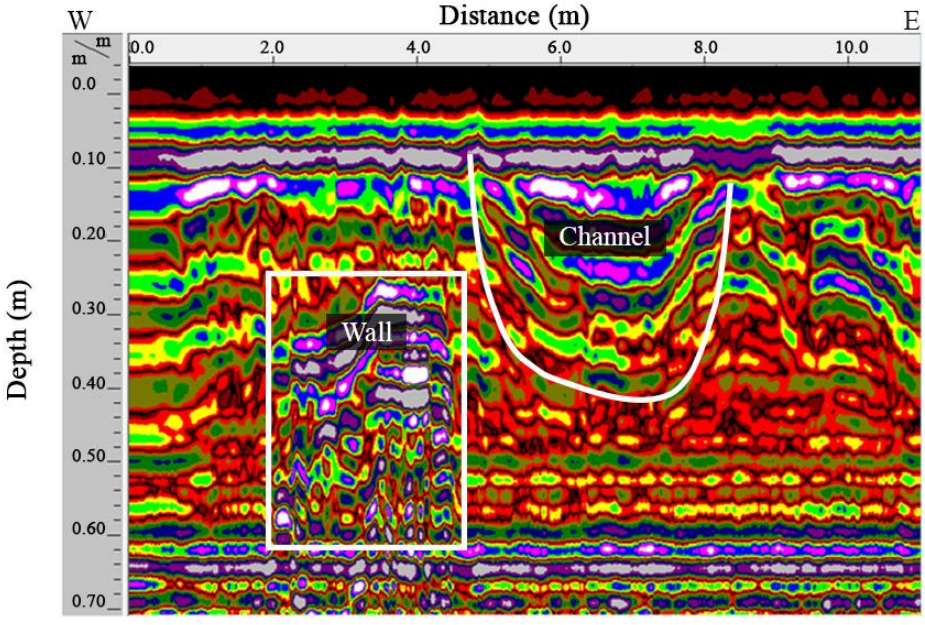

352
353
354 Figure-7

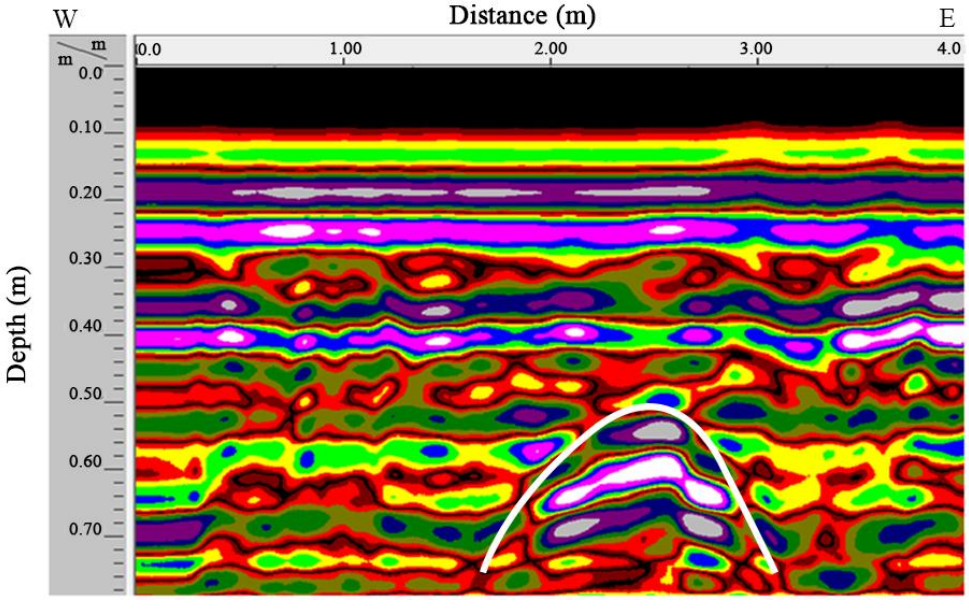

355
356
357 Figure-8
358

https://doi.org/10.5194/gi-2020-17
Preprint. Discussion started: 24 July 2020

Geoscientific Instrumentation Methods and Data Systems Discussions
Open Access
EGU

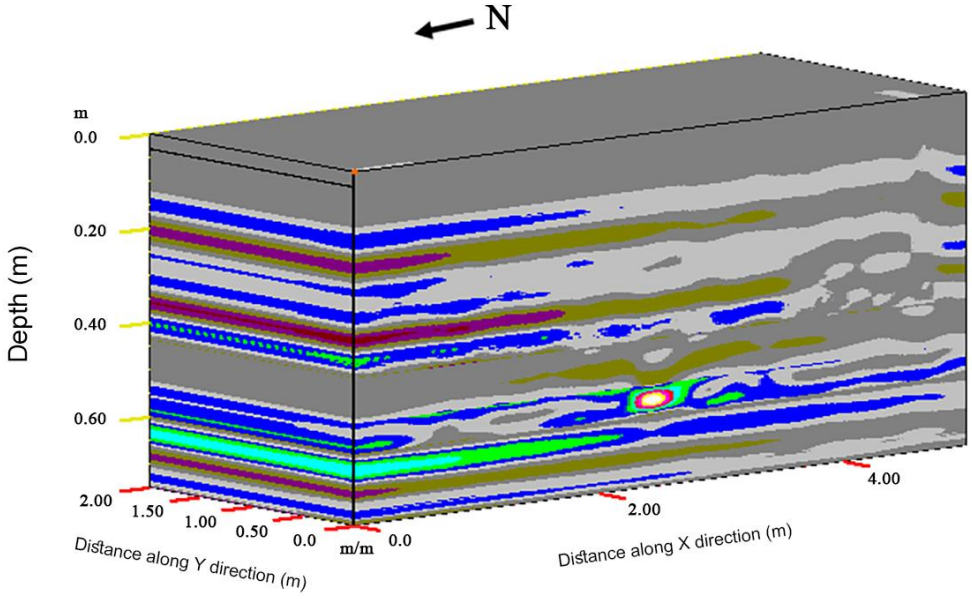

359
360 Figure-9
361

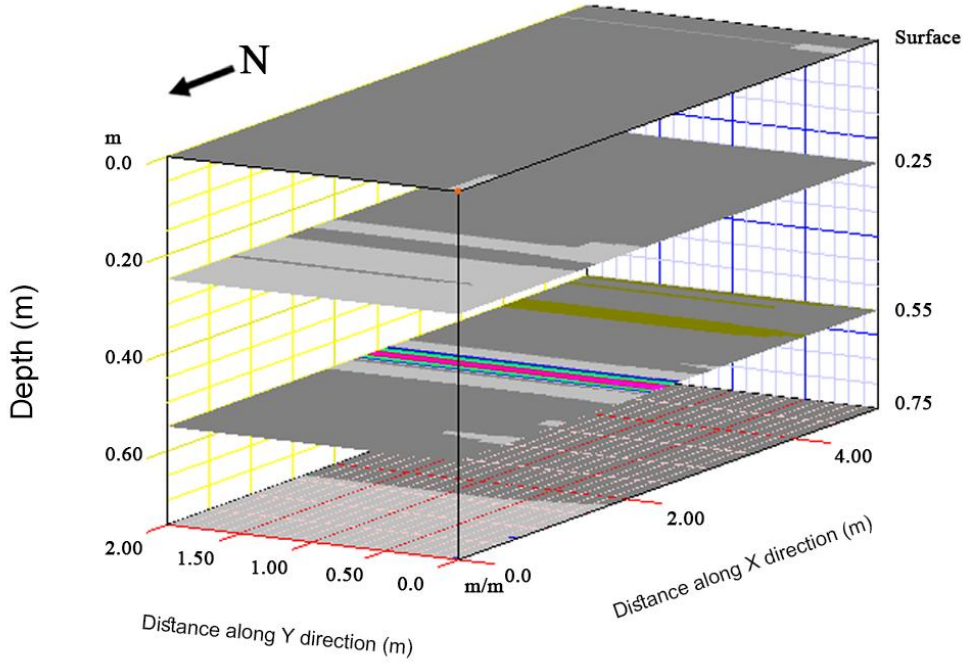

362
363 Figure-10
364

https://doi.org/10.5194/gi-2020-17
Preprint. Discussion started: 24 July 2020

Geoscientific Instrumentation Methods and Data Systems Discussions

365

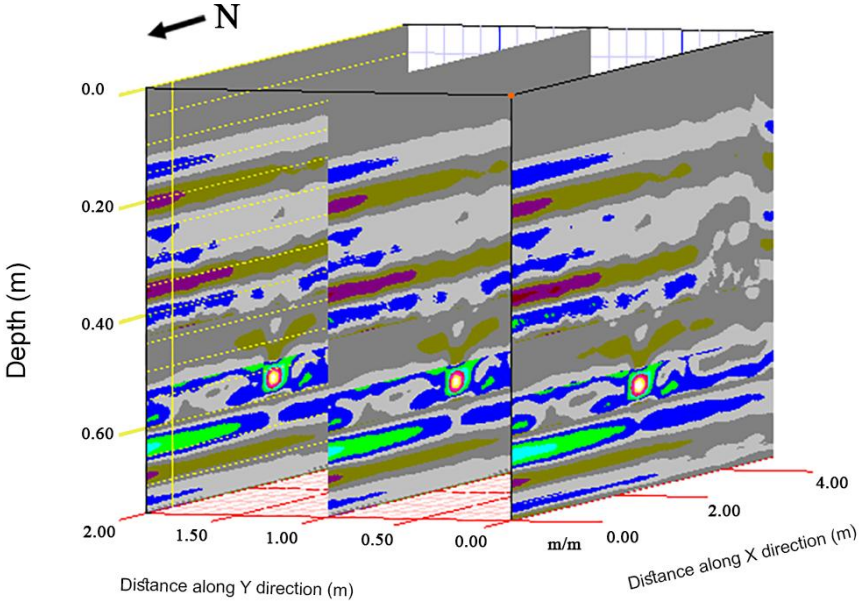

366
367 Figure-11
368

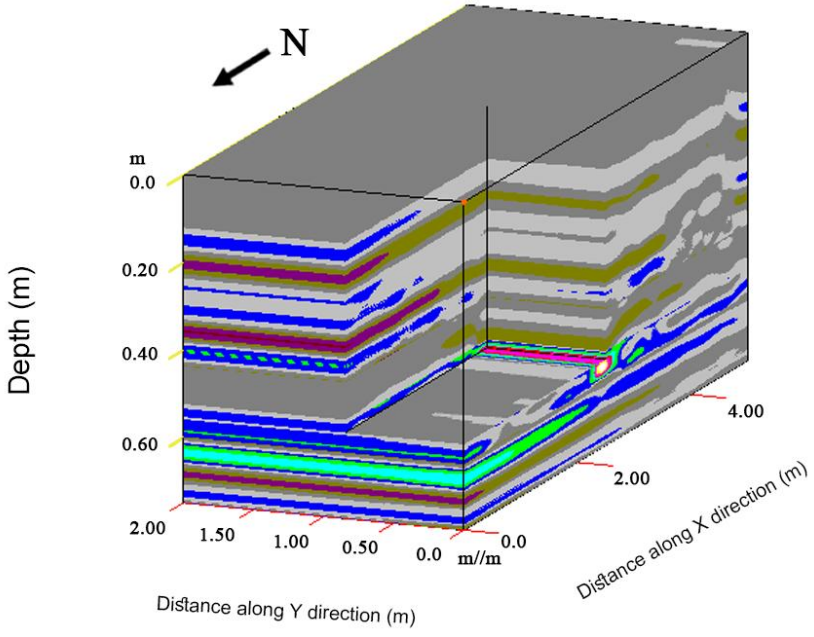

369
370 Figure-12

https://doi.org/10.5194/gi-2020-17
Preprint. Discussion started: 24 July 2020

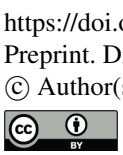

Geoscientific Instrumentation Methods and Data Systems Discussions
Open Access
EGU

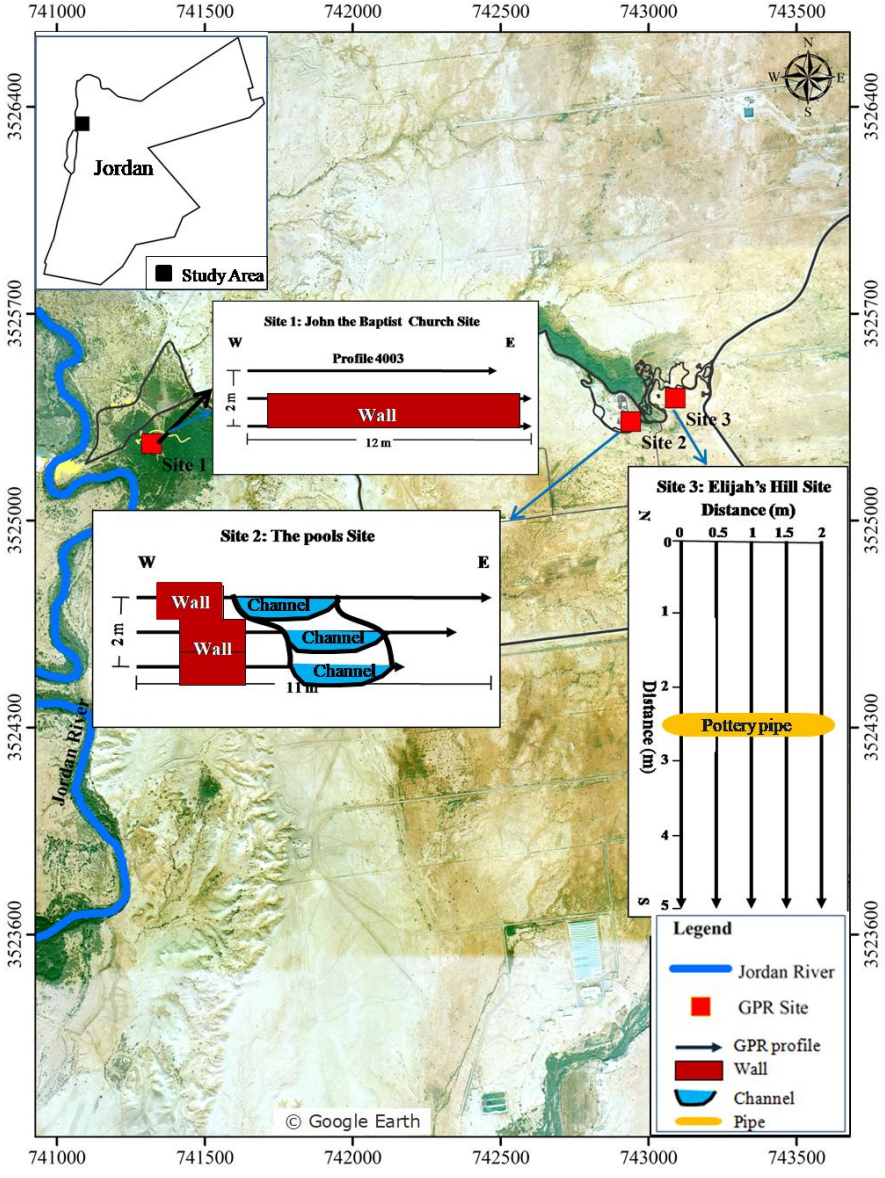

371
372 Figure-13

373

374

375

https://doi.org/10.5194/gi-2020-17
Preprint. Discussion started: 24 July 2020

Geoscientific Instrumentation Methods and Data Systems Discussions
Open Access
EGU

Figures Captures

Fig.1. Location map of the GPR profiles study area (After Google map).
Fig.2. Hyperbolic reflections caused by pottery pipe is used to obtain the wave velocity with the equation of hyperbola.
Fig.3. A 400 MHz antenna radargram along Profile4001. The white rectangle along the radargram at approximate depth of 1.2 m may correspond to buried wall.
Fig.4. A 400 MHz antenna radargram along Profile4002. The white rectangle along the radargram at approximate depth of 0.6 m may correspond to buried wall.
Fig.5. A 900 MHz antenna radargram along Profile9001. The white rectangle along the radargram represents anomaly located between horizontal distance 1 and 3 m with approximate depth 0.25 m which may correspond to an ancient buried wall. The 4 m wide depression at end of the profile may be correlated to buried channel.
Fig.6. A 900 MHz antenna radargram along Profile9002. The white rectangle along the radargram at approximate depth of 0.20 m may correspond to buried wall. The 4 m wide depression at end of the profile may be correlated to buried channel.
Fig.7. A 900 MHz antenna radargram along Profile9003. The white rectangle along the radargram at approximate depth of 0.20 m may correspond to buried wall. The 4 m wide depression at end of the profile may be correlated to buried channel.
Fig. 8 A part of 900 MHz antennae radargram along profile 1 immediately adjacent to excavated pottery pipe. The hyperbolic- shaped anomaly at distance 2.5 m and 0.55 m deep shows the extension location of the buried pottery pipe.
Fig. 9 The 3D GPR data view constructed from 2D profile lines. The 3D perspective view of processed profiles using high pass and low pass vertical and horizontal filters together with migration technique that show the location of the pottery pipe.
Fig.10. Depth slices with different depths (0, 025, 0, 55, 0.75 m) generated from 3D plot. The main anomaly observed with W-E direction at depth slice 0.55 mbs (meter below surface).
Fig.11. The multiple slices view along y direction at distance (0, 1 and 2 m) determines the depth and extension of the pipe.
Fig.12. The 3D section (cutout cube) using X=2.5 m, Y=0.85 m, and Z=0.55 m shows clearly the depth and extension of the pipe perpendicular to the X position and the depth of the top of pipe detect by the Z position.
Fig.13. Location map of the inferred archaeological material (after Google map)